

Characterization of Anatase Phase on Calcinated Titanium-V Alloy

M.D. Hamilton

Department of Biomedical Engineering, University of Michigan, Ann Arbor, Michigan

Arman Butt

Department of Bioengineering, University of Illinois at Chicago, Illinois

Sweetu Patel

Department of Bioengineering, University of Illinois at Chicago, Illinois

C. Sukotjo

Clinical Assistant Professor, Department of Restorative Dentistry, University of Illinois at Chicago, Illinois

C.G. Takoudis

Departments of Chemical Engineering and Department of Bioengineering, University of Illinois at Chicago, Illinois

1. Abstract

Surface modification of titanium implants has been a large focus of recent research. Thermal oxidation is a technique used to diffuse oxygen into the surface of a material to form an oxide layer. By varying the temperature of thermal oxidation, the crystal structure of the TiO₂ layer can be changed from amorphous to anatase. The crystal structure of anatase has been shown to resemble hydroxyapatite, a mineral that is involved in bone growth. FTIR, an Ellipsometer, and a Geonimeter are used to analyse the anatase concentrations created at 24, 300, 375, and 450 °C. It was found that hydrophilicity increases on rough samples as oxidation temperature increases. Also, a peak shift from anatase to rutile is seen as annealing temperatures increase in the range of 300 to 600 °C.

Keywords: Osseointegration, titanium oxide, anatase, thermal oxidation

2. Introduction

The goal of this experiment is to modify the implant surface such that it promotes osseointegration. A schematic of osseointegration is shown in Figure 1, detailing the progression of the bone-implant interface adhesion, which occurs when the natural bone connects to the implant surface. If this connection forms quickly, the implant has a greater possibility of remaining embedded, increasing the chance of success.^{1,2} However, without this connection, the implant becomes loose, loses functionality, and may become infected, leading to costly revision surgery.

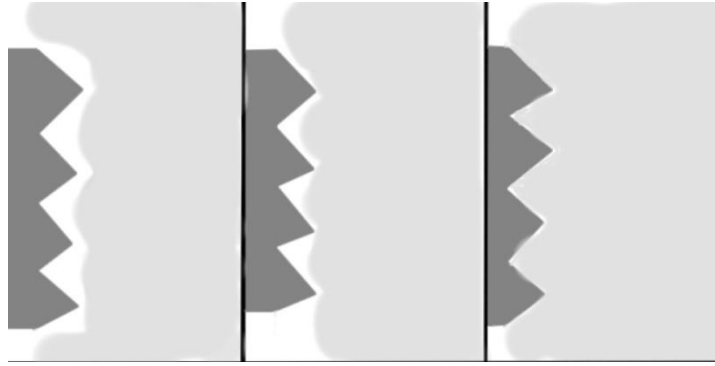


*Figure 1: Osseointegration → The bone integrates into the rough surface of the titanium implant.
Dark grey –Titanium screw implant. Light grey – bone.*

Titanium is a popular metal in the world of implants due to its excellent biocompatibility, low density, high ductility, corrosion resistance, atoxicity, and mechanical resistance.^{3,4} It is used mostly for dental and orthopedic implants. Commercially pure titanium does not have a tensile strength as high as some other implant materials such as cobalt-chromium. A widely used titanium alloy, Ti6Al4V, contains 6 w.t. % aluminum and 4 w.t. % vanadium. The combination of aluminum and vanadium with titanium makes the material stronger than the commercially pure titanium.^{3,5} Thus, this alloy is used with increasing frequency for dental and orthopedic purposes.

There is a possibility that Ti6Al4V can be cytotoxic when aluminum and vanadium ions dissociate from the bulk into neighboring tissues. Due to this and low wear resistance, surface modification is necessary for improved osseointegration.^{2,6} Sandblasting and acid-etching are techniques used to create a micro-rough surface.⁷ This roughened surface improves osseointegration by increasing the surface area for cellular attachment.⁸⁻¹⁰ Titanium forms an oxide layer (TiO₂) naturally, but it is advantageous to form an oxide layer under controlled conditions so that properties such as thickness and crystalline structure of the oxide layer can be controlled. Moreover, the varying oxide properties can be tested for superior osseointegration. The TiO₂ layer is advantageous because it increases biocompatibility and corrosion resistance.^{7,11}

Hydroxyapatite is a mineral found in the body that has been shown to enhance bone growth both naturally and when coated on implant surfaces.¹² In its anatase phase, TiO₂ has been found to assist in bone adhesion due to the similarities of its crystal structure to hydroxyapatite. The crystal structure of apatite alligns better with anatase than with rutile.¹³ In previous research, an anatase titanium nanotube surface has been shown to support cell growth better than an amorphous layer.^{6,14} As concentrations of antaste increase relative to rutile or amorphous, superior osseointegration is expected.

Thermal oxidation is a method used to diffuse oxygen into surfaces to create an oxide layer (See Figure 2). It has been shown that the roughness and thickness of the oxide layer increase with oxidation time.^{15,16} Thickness of the surface has also been shown to increase with the temperature to which the sample is exposed.¹⁵ Thermal oxidation was chosen over other techniques for various reasons: the oxide layer is conformal to surface topography, it is time efficient, and there is no precursor resulting in less contamination and lower cost. The oxide layer conforms better to the surface than chemical vapor deposition (CVD) or physical vapor deposition (PVD). Due to the diffusion mechanism, the oxide layer conforms to the roughness created by sandblasting and acid etching. Thermal oxidation is more time efficient when

compared to atomic layer deposition (ALD). For example, depositing a 30 nm thick layer would take 16 hours at reported 0.3Å/cycle/minute as opposed to one hour for thermal oxidation at ambient conditions and 550 °C.^{15,17} There is no precursor needed for thermal oxidation unlike CVD, PVD, and ALD, reducing impurities and cost.

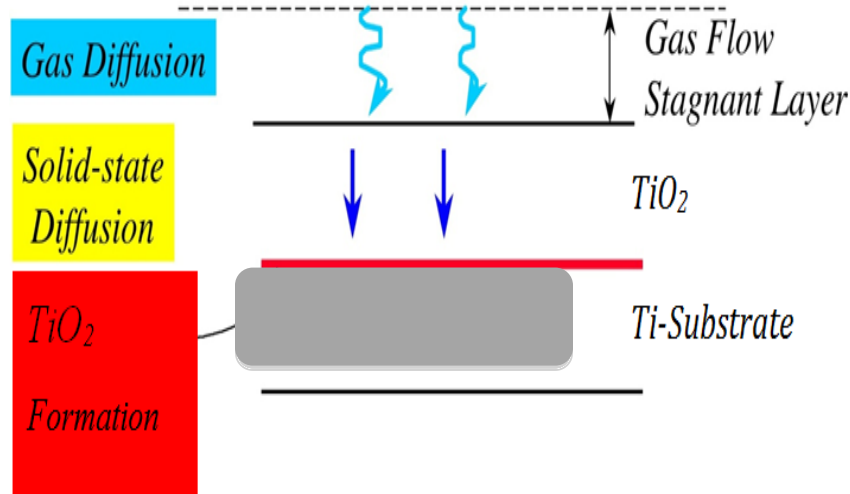


Figure 2: This schematic shows the formation of TiO₂ due to the diffusion of O₂ into the surface of the titanium substrate.

3. Materials and Methods

A Single-zone Quartz Oxidation/Nitridation/Oxynitridation Furnace (Lindberg, S#848040) was used to oxidize the Ti6Al4V samples at different temperatures. The oxidation tube is made of quartz. The furnace facilitates the diffusion of oxygen into the surface at atmospheric air and ambient pressure. The setup of the system can be seen in Figure 3.

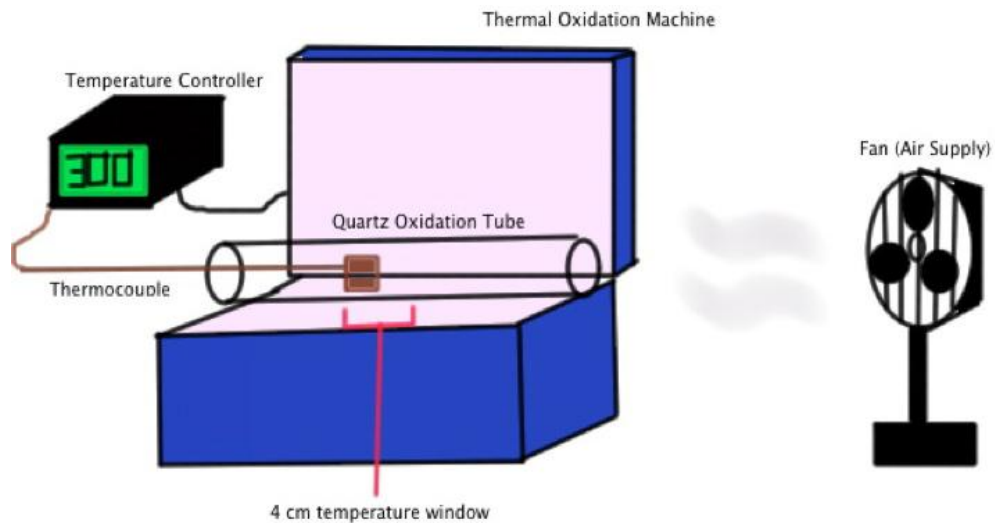


Figure 3: The inside of the thermal oxidation furnace. The schematic of the fan, thermocouple, and temperature controller.

Four samples annealed at different temperatures were surface modified and tested with Fourier Transform Infrared Spectroscopy (FTIR, Nicolet. S#ADU9700221), a Goniometer (Rame'-Hart NRL CA. M#100-0, S#2067), and an Ellipsometer (J.A. Woollam Co. M-44). The control samples were oxidized at the ambient temperature of 24 °C, thus the sample was not be annealed. This was expected to create a TiO₂ layer in the amorphous phase. The three other temperatures were 300, 375, and 450 °C. Two additional samples were made and thermally oxidized at 525 °C and 600 °C. These two temperatures were done for to see a peak shift towards rutile during FTIR. Anatase phase has been shown form between the thermal oxidation temperatures of about 250 – 500 °C.^{15,18,19} The amount of anatase is expected to be greater towards the middle of this range. Therefore, the thermally oxidized samples at 300 – 450 °C were expected to contain varying concentrations of anatase.

Ti6Al4V samples (Mac-Master Carr, Elmhurst, IL, USA) of 15 mm diameter and 1 mm thickness first had their surfaces modified. To create the smooth samples, eight samples were polished using a polishing wheel (Ecomet Polisher/Grinder, Buehler LTD, Evanston, IL, USA) with Special Silicon Carbide Grinding Paper for Metallography Wet or Dry (#320, #400, #600, #800. Buehler, 0/1102), Diamond Polishing Paste (Buehler, 9-Micron, 487597), MetaDi Fluid (Buehler, 499594), and Colloidal Silica Polishing Suspension (MasterMet. Buehler, 40-6370-064). To create the rough samples, eight samples were sandblasted (Renfert Sandblaster) with 165-micrometer diameter alumina (Al₂O₃) particles and acid-etched with a 1:1 ratio of hydrogen peroxide that was 30 w.t. % solution by water and sulfuric acid. The rough samples were then sonicated in deionized water. Before thermal oxidation, each sample was washed with deionized water for 30 seconds and then dried with nitrogen gas. Additional rough samples were made for a continuation of this experiment to measure the cell viability of the thermally oxidized samples at the four temperatures.

Once thermal oxidation was complete and the sample cooled to room temperature, the sample could then be characterized. Ellipsometry was used to measure the thickness of the oxide layer. Due to the multiple suboxides that are created in addition to TiO₂ such as TiO and Ti₂O₃, ellipsometry can only provide an approximate thickness.^{20,21} Therefore, to supplement the ellipsometric data, the color of the sample was also taken into account. Previously, the correlation between color and oxide thickness has been investigated as shown in Table 1. FTIR iwas used to measure chemical composition to test for impurities and to determine the relative amounts of amorphous, anatase, and rutile TiO₂. A Goniometer was used to measure the water contact angle (WCA), a measure of hydrophilicity. Previous research has shown that increasing oxidation temperatures increases surface roughness, which increases the hydrophilicity of the surface.²² To a limitation, surfaces that are more hydrophilic have been shown to increase cell growth.²³ Anatase structure, oxide thickness, and surface roughness have all been shown to affect cellular response and thus need to be taken into account when interpreting future cell test results.^{15,22,24}

| Layer Thickness (nm) | 10-25 | 25-40 | 40-50 | 50-80 | 80-120 | 120-150 | 150-180 | 180-210 |
|----------------------|--------|--------|-----------|------------|--------|---------|---------|---------|
| Color | Golden | Purple | Deep Blue | Light Blue | Yellow | Orange | Purple | Green |

Table 1: Colors of Oxide Layer After Anodic Oxidization.¹⁵ This shows the relationship between oxide layer color and thickness.

4. Results and Discussion

4.1. Goniometer

The Goniometer was used to measure water contact angle. It was used on the smooth and rough samples. Results of the tests can be seen in Figure 4. At 375 °C, the rough sample is missing due to experimental error. It was determined from this error that the samples should not be washed prior to testing with the Goniometer because this makes the sample superhydrophilic, making the differences in hydrophilicity between samples impossible to detect. The smooth samples show a slight decrease in water contact angle as temperature increases, but the trend is not convincing. The rough samples have a clear trend, increasing in hydrophilicity as the oxidation temperature increases. This agrees with previous research.²² It can also be seen that at a higher temperature (450 °C), the rough sample is more hydrophilic, agreeing with literature.²² According to this data, a micro-rough surface oxidized at 450 °C will be more hydrophilic than a smooth sample or a rough sample oxidized at a lower temperature.

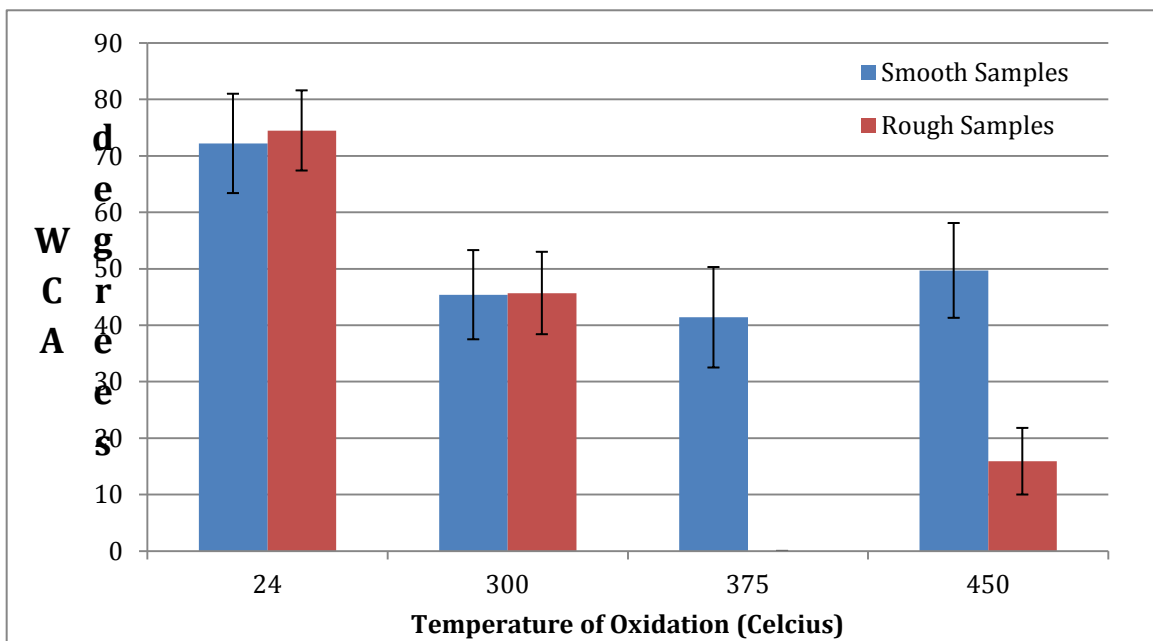


Figure 4: Temperature of oxidation vs. water contact angle. The smooth samples are shown in blue and the rough samples in red. Water contact angle is a measure of hydrophilicity. Hydrophilicity increases with increasing oxidation temperature for rough samples.

4.2. Color Characterizations

Color characterizations were conducted in place of ellipsometry. Observations of color were referenced from literature (Table 1). Table 2 shows the estimated oxide layer thickness based on color observations. According to the estimations, the thickness of the oxide layer increases with

temperature at which the samples were annealed. Samples do not show a color change until 450 °C. The exponential increase in thickness seen at 600 °C agrees with literature.¹⁵

| Temperature (°C) | 24 | 300 | 375 | 450 | 525 | 600 |
|---|------|------|-------------|-------------|--------------|---------------|
| Observed Color | None | None | Slight Gold | Golden | Yellow | Purple-blue |
| Estimated TiO ₂ Thickness (nm) | <10 | <10 | 10 < x < 25 | 10 < x < 25 | 80 < x < 120 | 150 < x < 210 |

Table 1: This shows the various temperatures at which smooth samples were thermally oxidized and the estimated thicknesses of the oxide layers based on the observable colors.

4.3. Fourier Transform Infrared Spectroscopy

FTIR was done for temperatures 300-600 °C. The control, 24 °C, was used as the background for the FTIR data. Figure 5 shows a match scale version of the FTIR data. The main peak between 830 and 870 cm⁻¹ is representative of TiO₂. The amplitude and area of the peak correlates with the intensity of the FTIR scan. This intensity is representative of TiO₂ thickness. Thus, the higher the peak, the thicker the TiO₂ layer. It can be seen that the height of the peak increases with annealing temperature. The peak at 300 °C is shortest and the peak at 600 °C is tallest. As previous research has stated, the thickness of the oxide layer increases with annealing temperature and this trend can be observed in Figure 5.¹⁵

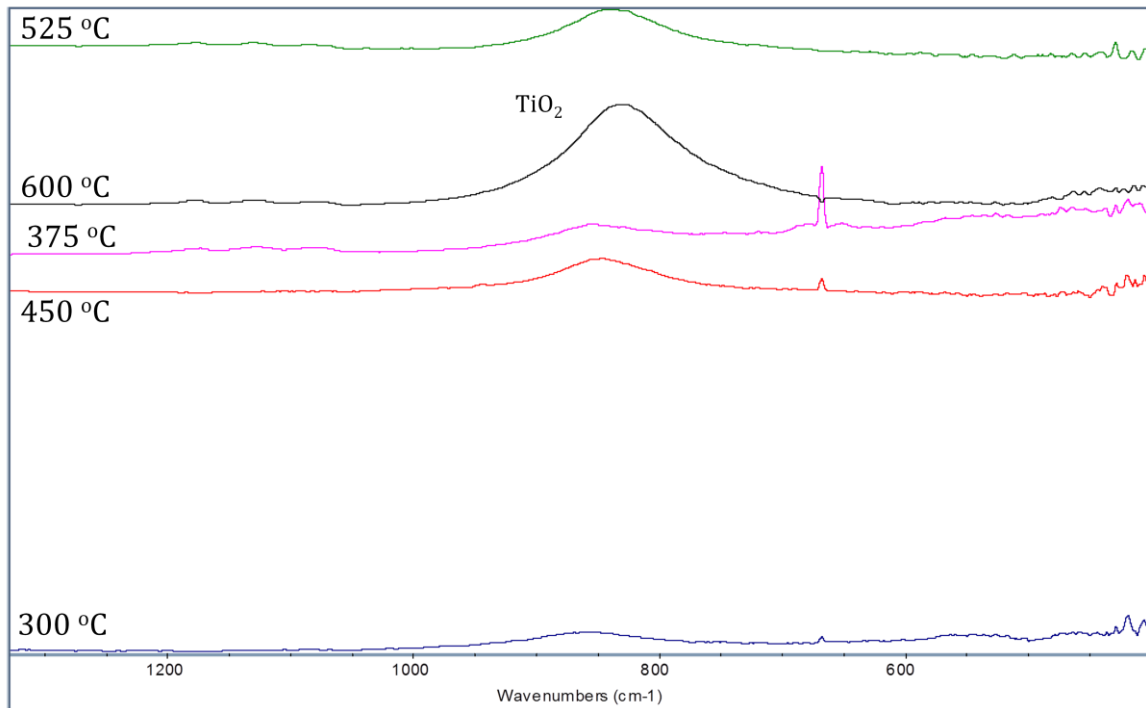


Figure 5: FTIR graphs for temperatures 300 (blue), 375 (magenta), 450 (red), 525 (green), and 600 °C (black). The increasing height of the peak indicates an increasing thickness of TiO₂.

A close-up of the TiO_2 peak from Figure 5 can be seen in Figure 6. The most prominent peak is TiO_2 , which is made up of both anatase and rutile phases. The anatase and rutile peaks are indistinguishable, but the relative amounts of anatase compared to rutile can be seen through the shift in the TiO_2 peak. In literature, anatase is seen at 870 cm^{-1} and 550 cm^{-1} and rutile is seen at 830 cm^{-1} . At lower temperatures (300 and $375\text{ }^\circ\text{C}$), the TiO_2 peak is more toward 870 cm^{-1} (anatase). At higher temperatures (450 , 525 , and $600\text{ }^\circ\text{C}$), the peaks can be seen more toward 830 cm^{-1} (rutile). This shows the shift of the peak from anatase to rutile as annealing temperature increases. Anatase can also be seen at 550 cm^{-1} for 300 and $375\text{ }^\circ\text{C}$, further showing the formation of relatively higher amounts of anatase at lower temperatures within this range. Peaks in the anatase range at lower temperatures and a gradual shift towards rutile was seen and expected.¹⁵

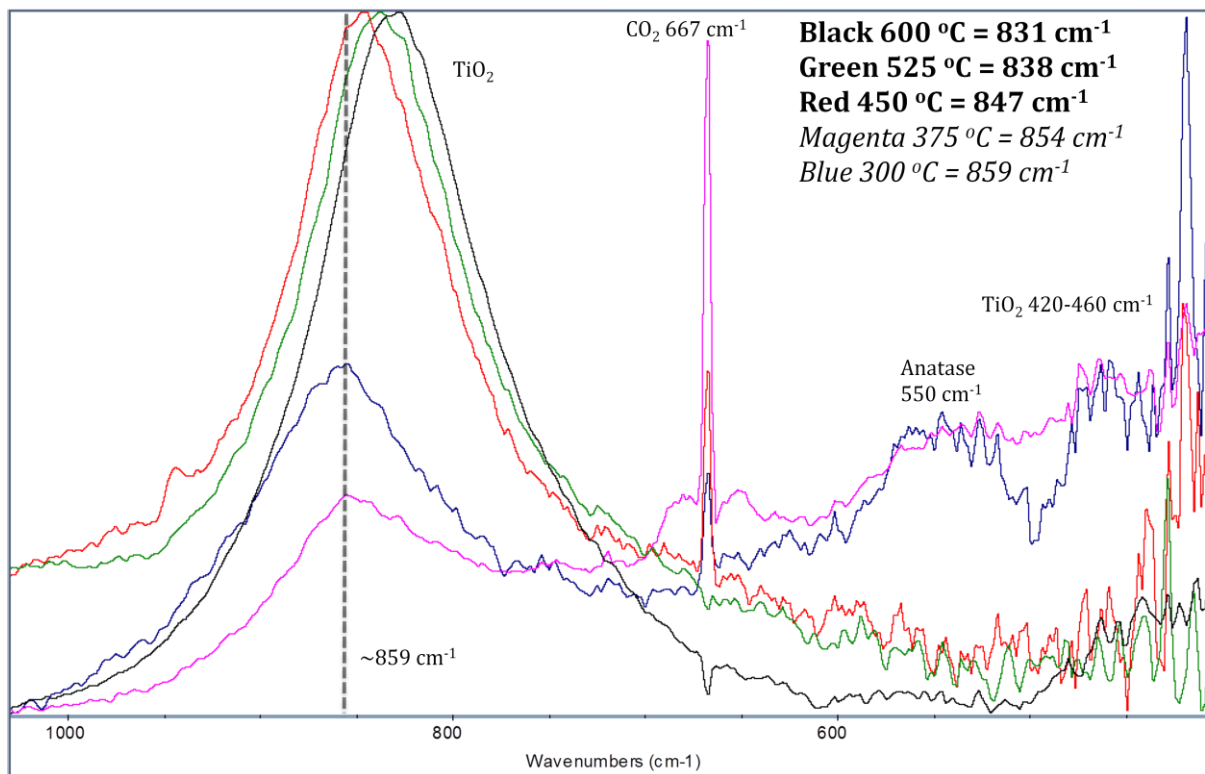


Figure 6: FTIR data for temperatures 300 (blue), 375 (magenta), 450 (red), 525 (green), 600 (black) $^\circ\text{C}$. This shows the shift from anatase to rutile TiO_2 as the annealing temperature increases.

5. Conclusion

The results of this experiment correlated well with literature. It was successfully shown that oxide thickness increases with increasing thermal oxidation temperature. It was also shown that, for rough samples, surface hydrophilicity increases with oxidation temperature; this was not seen for smooth samples. Through FTIR, it was shown that anatase exists in the range $300 - 450\text{ }^\circ\text{C}$ as the primary crystalline structure. The shift from anatase to rutile with the increasing temperature was shown in the FTIR scans.

For future work, more samples and more temperatures should be tested to improve the precision of the anatase to rutile shift. Also, using X-Ray Diffraction (XRD) would allow for better observation of the individual crystal structure peaks. In a continuation of this project, Santiago Tovar will continue with cell culture assay. He will relate the characterizations done in this experiment to the cell assay results.

6. Acknowledgements

The authors would like to thank the National Science Foundation EEC-NSF Grant # 1062943 for funding the Research Experience for Undergraduates. The authors would also like to thank Dr. Jursich, Dmitry Royhman, and Santiago Tovar for supervising, advising, and assisting this experiment.

7. References

- [1] P.R. Klokkevold, R.D. Nishimura, M. Adachi and A. Caputo: *Clin. Oral Impl. Res.*, 1997, 8, 442-447.
- [2] M. Geetha, A.K. Singh, R. Asokamani and A.K. Gogia: *Progress in Materials Science*, 2009, 54, 397-425.
- [3] R. Van Noort: *Journal of Materials Science*, 1987, 22, 3801-3811.
- [4] S. Bruni, M. Martinesi, M. Stio, C. Treves, T. Bacci and F. Borgioli: *Acta Biomaterialia*, 2005, 1, 223-234.
- [5] M. Rinner, J. Gerlach and W. Ensinger: *Surface and Coatings Technology*, 2000, 132, 111-116.
- [6] S. Minagar, C. C. Berndt, J. Wang, E. Ivanova, C. Wen: *Acta Biomaterialia*, 2012, 8, 2875-2888.
- [7] L.H. Li, Y.M. Kong, H.W. Kim, Y.W. Kim, H.E. Kim, S.J. Heo and J.Y. Koak: *Biomaterials*, 2004, 25, 2867-2875.
- [8] E. Nasatzky, B. Boyan and Z. Schwartz: *The Alpha Omegan*, 2005, 98, 9-19.
- [9] M.R. Khan, N. Donos, V. Salih and P.M. Brett: *Bone*, 2012, 50, 1-8.
- [10] J. H. Park, Z. Schwartz, R. Olivares-Navarrete, B. D. Boyan and R. Tannenbaum: *Langmuir*, 2011, 27, 5976-5985.
- [11] J. Pouilleau, D. Devilliers, F. Garrido, S. Durand-Vidal and E. Mahe: *Materials Science and Engineering*, 1997, B47, 235-243.
- [12] M. Hirota, T. Hayakawa, M. Yoshinari, A. Ametani, T. Shima, Y. Monden, T. Ozawa, M. Sato, C. Koyama, N. Tamai, T. Isai and I. Tohnai: *Int. J. Oral Maxillofac. Surg.*, 2012, article in press.
- [13] M. Uchida, H.M. Kim, T. Kokubo, S. Fujibayashi and T. Nakamura: *J. Biomed. Mater. Res.*, 2002, 64A, 164-170.
- [14] S. Oh, C. Daraio, L.H. Chen, T.R. Pisanic, R.R. Finones and S. Jin: *Wiley Periodicals, Inc. J. Biomed. Mater. Res.*, 2006, 78A, 97-103.
- [15] D. Velten, V. Biehl, F. Aubertin, B. Valeske, W. Possart and J. Breme: *J. Biomed. Mater.*, 2002, 59, 18-28.
- [16] H. Güleriyüz and H. Çimenoglu: *Biomaterials*, 2004, 25, 3325-3333.
- [17] R. Katamreddy, V. Omarjee, B. Feist and C. Dussarrat: *ECS Transactions*, 2008 16, 113-122.

- [18] H. Tang, K. Prasad, R. Sanjines, P.E. Schmid, and F. Levy: *Journal of Applied Physics*, 1994, 75, 2042-2047.
- [19] E. Gemelli and N. H. A. Camargo: *Revista Matéria*, 2007, 12, 525-531.
- [20] F. Variola, J. Yi, L. Richert, J. D. Wuest, F. Rosei, A. Nanci: *Biomaterials*, 2008, 29, 1285-1298.
- [21] E. McCafferty, J. P. Wightman: *Applied Surface Spectroscopy*, 1999, 143, 92-100.
- [22] F. Rupp, L. Scheideler, D. Rehbein, D. Axmann and J. Geis-Gerstorfer: *Biomaterials*, 2004, 25, 1429-1438.
- [23] P. B. van Wachem, T. Beugeling, J. Feijen, A. Bantjes, J. P. Detmers and W. G. van Aken: *Biomaterials*, 1985, 6, 403-408.
- [24] B.E. Deal and A.S. Grove: *J. Appl. Phys.*, 1965, 36, 3770-3778.